

1 Meteorological factors driving glacial till variation and the associated
2 periglacial debris flows in Tianmo Valley, southeast Tibetan Plateau

3 M. F. Deng^{1,2}, N. S. Chen^{1*}, and M. Liu^{1,2}

4 (¹ Key Laboratory of Mountain Hazards and Surface Process, Institute of Mountain Hazards and Environment,
5 Chinese Academy of Sciences, Chengdu 610041, China;

6 ² University of Chinese Academic of Sciences, Beijing 100049, China)

7 Abstract: Meteorological studies have indicated that high Alpines are strongly affected by climate
8 warming. Periglacial debris flows are frequent in deglaciated regions. The combination of rainfall
9 and air temperature controls the initiation of periglacial debris flows; and the addition of
10 melt-water due to higher air temperatures enhances the complexity of the triggering mechanism
11 compared to storm-induced debris flows. In south-eastern Tibetan Plateau where temperate
12 glaciers are widely distributed, numerous periglacial debris flows have occurred in the past 100
13 years, but none had happened in the Tianmo watershed until 2007. In 2007 and 2010, three
14 large-scale debris flows occurred in the Tianmo watershed. In this research, these three debris flow
15 events were chosen to analyze the impact of the annual meteorological conditions: the antecedent
16 air temperature and meteorological triggers. TM images and field measurement of the nearby
17 glacier suggested that a sharp glacier retreat had existed in the previous one or two years
18 preceding the events, which coincided with the spiked mean annual air temperature. Besides,
19 changing of glacial tills driven by prolonged increase in the air temperature is the prerequisite of
20 periglacial debris flows. Triggers of periglacial debris flows are multiplied and they could be high
21 intensity rainfall as in first debris flows and the third debris flows, or continuous long term rising
22 air temperatures as in the second debris flows.

23 Key words: glacial till variation; meteorological factors; periglacial debris flows;
24 southeast Tibetan Plateau

25 **1. Introduction**

26 The alpine environments are strongly vulnerable to climate changes, of which the
27 alpine glaciers and permafrost are the most sensitive in the form of glacier and
28 permafrost degradation (Harris et al, 2009; IPCC, 2013). Glacier and permafrost retreat
29 can induce mass movement, such as landslides, shallow slides, debris, moraine
30 collapses, etc. (Cruden and Hu, 1993; Korup, 2009; McColl, 2012; Stoffel and Huggel,
31 2012; Fischer et al, 2012), that will be expelled out of the watershed in the form of

32 debris flows or sediment flux. The debris flow in alpine areas can often bury
33 residential areas, cut off main roads and block rivers (Shang et al, 2003; Cheng et al,
34 2005; Deng et al, 2013) and destroy basic facilities located in downstream, posing a
35 great threat to the local economy and social development. In undeveloped alpine areas
36 such as the south-eastern Tibet where the transportation system is particularly poor or
37 limited, the negative effects produced by debris flows such as cutting off main roads
38 are serious (Cheng et al, 2005).

39 Periglacial debris flows occurs in the high alpine areas where there is large areas
40 of glaciers, such as the Tibetan Plateau in China(Shang et al, 2003; Ge et al, 2014),
41 Alps in Europe(Sattler et al, 2011; Stoffel and Huggel,2012), Caucasus Mountains in
42 Russia(Evans et al, 2009) and Andes in northern Canada(Lewkowicz1 and Harris,
43 2005). Periglacial debris flows were reported to be initiated by rainfall (Stoffel et al,
44 2011; Schneuwly-Bollschweiler and Stoffel, 2012), melt-water flow of glacier or ice
45 particle ablation(Arenson and Springman, 2005; Decaulne et al, 2005), or outburst
46 floods from glacier lakes (Chiarle et al, 2007) in different parts of the world, while the
47 multi-triggers for the case is rarely to be read. Because debris flows are commonly
48 triggered by rainfall (Sassa and Wang, 2005; Decaulne et al, 2007; Kean et al, 2013;
49 Takahashi, 2014), the rainfall threshold, intensity and duration has been widely used
50 for debris flow monitoring and giving warning in non-glacier areas (Guzzetti et al,
51 2008).

52 In deglaciation areas, the debris flow threshold can be more difficult to determine.
53 Periglacial debris flows tend to occur in the summer when the thawing of glaciers and
54 glacial tills predominates and melt-water penetrates into the glacial tills at a constant
55 and successive flow. The effect of melt-water appears similar to that of antecedent
56 rainfall (Rahardjo et al, 2008) and is variable in different periods, considering snow
57 and glacier shrinkage and air temperature fluctuation. In the Swiss Alps, melt-water is
58 high in early summer, and as debris flows can be initiated by low total rainstorm,
59 whereas higher total rainstorm are required in late summer or early autumn when the
60 melt-water is low (Stoffel et al, 2011; Schneuwly-Bollschweiler and Stoffel, 2012). In
61 south-eastern Tibetan Plateau, the rainfall threshold given by Chen et al., (2011) is

62 quite wide, and the small rainfall threshold in particular is likely to contain the effect
63 of air temperature. Moreover, periglacial debris flows induced by a sudden release of
64 water from glacier lakes have a close relationship with the rising air temperature (Liu
65 et al, 2014).

66 Fluctuation of air temperature is likely to be quite important in triggering
67 periglacial debris flows. Compared with the storm induced debris flows, the addition
68 of air temperature can greatly enhance the complexity of the initiation of periglacial
69 debris flows. It is of high difficulty to simulate the triggering process by experiment
70 or mathematical simulation, and instead, debris flows cases in the natural environment
71 could be applied. In this research, three debris flow events, after a debris-flow-free
72 period of nearly 100-year, in the Tianmo watershed of the southeastern of the Tibetan
73 Plateau as deglaciation continued are used as examples, and the annual meteorological
74 conditions, antecedent air temperature and triggering conditions prior to debris flows
75 are analyzed to further understand the meteorological triggers and their roles in
76 glacier retreat, glacial till variation and debris flow initiation.

77 **2. Background**

78 **(1) Study area**

79 The temperate glacier in the Tibetan Plateau is primarily distributed in the
80 Parlung Zangbo Basin and covered a total landmass of 2381.47 km² in 2010 based on
81 TM images (Liu, 2013). Historically, the movement of temperate glacier has produced
82 a large amount of moraines, the depth of which can reach up to 500 m locally (Yuan et
83 al, 2007). In recent decades, there has been a dynamic significant increase in
84 temperature and according to statistics the temperature at the Bomi meteorological
85 station (midstream in the Parlung Zangbo Basin) has rose by 0.23°C/10a from 1969 to
86 2007, resulting in remarkable shrinkage of the glacier(Yang et al, 2010).

87 Tianmo Valley, located in Bomi County and to the south of the Parlung Zangbo
88 River, covers an area of 17.76 km² (29°59'N/95°19'E; Figure 1). This valley has a
89 northeast-southeast orientation and is surrounded by high mountains reaching 5590 m

90 a.s.l. at the southernmost site and 2460 m a.s.l. at the junction of the Parlung Zangbo
91 River. The TM image in 2013 showed the presence of a hanging glacier with an area
92 of 1.42 km² in the upper concave area at an altitude of 4246 m to 4934 m. Bared rock,
93 dipping at an angle of around 60°, emerged below and above the hanging glacier and
94 often covered by everlasting snow. Below 3800m a.s.l., vegetation, including forest
95 and shrub, occupies most of the area (Table 1).

96 The river channel in the watershed is sheltered by shade and not directly affected
97 by sunlight, resulting in less solar radiation and a location at which a small trough
98 glacier can form. In the main channel, the trough glacier extended to 2966 m a.s.l. in
99 2006. The lower part of the trough glacier has been eroded by glacier melt-water flow,
100 and an arch glacier that is vulnerable to high pressure was formed (Figure 2). The
101 remnants of the landslide deposits approximately 10 meters high, which consist of low
102 stability sediment and can be easily entrained by debris flows, can be observed in both
103 sides of the channel.

104 Tianmo Valley is on the north side of the bend in the Yarlung Zangbo River and
105 is strongly affected by the new tectonic movement. An inferred normal fault vertical
106 to the channel cuts through the valley and is only 30 km away from the Yarlung
107 Zangbo fault. In 1950, a rather significant earthquake (Ms. 8.6) hit Zayu, which is
108 only 200 km away, and local records reported that a large amount of rock collapsed
109 and landslides were produced at that time. The whole valley is in a strong ductile
110 deformation zone and is dominated by gneissic lithology belonging to Presinian
111 System.

112 **(2) Disaster history**

113 According to our field interview with local residents, there were no debris flows
114 in approximately 100 years prior to 2007 in Tianmo Valley. The channel was quite
115 narrow before 2007, and the local people could walk across via a wooden bridge to
116 live and farm on the terrace on the west side.

117 On the morning of Sep. 4th, 2007, after the rainfall which did not hit the
118 downstream area ceased, the local forest guard heard a loud noise coming from the

119 upstream area at approximately 18:00; with rainfall which later began in the upstream
120 area at approximately 19:00, following this rainfall was debris flows which rushed out
121 of the Tianmo Channel and subsequently blocked the Parlung Zangbo River; report
122 stated that several debris flows occurred, lasting the entire night. According to the
123 field measurements, approximately 1,340,000 m³ of sediment was transported during
124 this event, resulting in 8 missing persons and deaths. Concurrently within this same
125 time, debris flows occurred in the four nearby valleys (Table 2). According to the size
126 classification proposed by Jakob (2005), which is based on the total volume, peak
127 discharge and inundated area, Size class of debris flows in the five valleys is given in
128 Table 2. This debris flows is listed as DF1 in this paper.

129 At 11:30 on Jul. 25th, 2010, debris flows were again triggered in Tianmo Valley
130 that traced the path of the preceding debris flow deposits and reached the other side of
131 the Parlung Zangbo River. According to Ge et al., (2014), solid mass sediment of
132 approximately 500,000 m³ was carried out (Table 1) and deposited on the cone to
133 block the main river. A barrier lake was formed, and the rising water destroyed the
134 roadbed of G318. The following week also experienced dozens of debris flows in
135 small magnitude. This debris flows is listed as DF2 in this paper.

136 Debris flows occurred again two months later on Sep. 6th (The Ministry of Land
137 and Resources P. R. C., 2010), although we could not determine the exact times
138 sequence of event but according to speculation, these debris flows could have
139 occurred in the early morning before dawn and when the rainfall intensity has reached
140 its maximum(Figure 9), which agrees with the findings of Chen (1991) that periglacial
141 debris flows have historically occurred between 18:00~24:00 in this area. The debris
142 barrier in the main river was consequently increased by an additional 450,000 m³, and
143 the barrier lake was enlarged to maintain 9,000,000 m³ of water. This debris flows is
144 listed as DF3 in this paper.

145 A field investigation revealed that a high percentage of boulders in the
146 downstream area and glacial tills above the trough glacier were quite loose and of
147 high porosity (Figure 2), hence they have low density and can be easily entrained. Our
148 particle size tests on the glacial tills and debris flow deposits indicate a lower clay

149 (d<0.005 mm) content, whereas the debris flow deposits contain more fine particles
150 that are smaller than 10 mm (Figure 4), suggesting that the entrainment supplied a
151 considerable amount of fine particles.

152 **(3) Meteorological data**

153 The study area is located in a high alpine area where the economy is quite
154 undeveloped with only few meteorological stations. Before 2011, the Bomi
155 meteorological station(since 1955) was the only station in the area, located 54 km
156 away from Tianmo valley at an altitude of 2730 m, and other stations were located
157 more than 200 km away.

158 The Tibetan Plateau is a massive terrace that obstructs the Indian monsoon,
159 causing it to travel through the Yarlung Zangbo Canyon and its tributaries. As the
160 Indian monsoon is transported to higher altitudes, a rainfall gradient emerges in the
161 Parlung Zangbo Basin. However, according to our statistics on rainfall data in the area,
162 the rainfall often enjoys the similar intensity for the long-term rainfall process from
163 Guxiang to Songzong which means there is no large rainfall gradient between
164 Tianmo valley and Bomi meteorological station; therefore, the rainfall data from the
165 Bomi meteorological station can be used for our study for the long duration rainfall
166 process. In order to conduct further study, another meteorological station was built in
167 2011 near Tianmo Valley.

168 It has been established that the air temperature decreases with altitude; therefore
169 the air temperature in the source area of Tianmo Valley is lower than that in Bomi
170 County. According to the research by Li and Xie (2006), the air temperature decreases
171 at a rate of (0.46~0.69)°C/100m over the whole Tibetan Plateau, and the rate in the
172 study area is 0.54°C/100 m. Because the glacier and permafrost in the source area
173 have a planar distribution, the air temperature at the geometric centre of the glacier
174 and permafrost can be used to analyze the temperature process.

175 **3. Analysis and results**

176 **(1) Changing of air temperature and rainfall**

177 The mean annual air temperature is usually used to reflect the tendency of glacier
178 change (Yang et al, 2015). We collected the mean annual air temperature and annual
179 rainfall data from 1970 to 2014 from the Bomi meteorological station (Figure 5). The
180 record showed that the mean air temperature has increased by approximately 1.5°C in
181 the last 45 years, accounting for 0.033°C/a. This air temperature increase was
182 particularly more rapid between 2005~2007, an approximately 0.7°C/3a, which is 7
183 times the average value of the last 45 years. On the other hand, the annual rainfall
184 from 2000 to 2010 was low and it was estimated at 828.2 mm per year. From 2000 to
185 2004, the rainfall during summer (July to September) accounted for approximately 50%
186 of the total annual rainfall; however, only 32% of the rainfall occurred in the summer
187 of 2005~2006, even though the annual rainfall exhibited the same trend. In 2007,
188 rainfall in the summer and the entire year returned to the mean rainfall state.

189 According to Figure 5, a similar trend in the air temperature and rainfall was
190 observed before DF2 and DF3. The air temperature elevated in 2009 to reach the
191 maximum of the last 45 year period, accounting for 10.2 °C; however, the annual
192 rainfall, was only 65% of the average amount; and the summer rainfall, lower than
193 that in 2005 and 2006, reached their minimum values. In 2010, the rainfall was
194 abundant and the annual rainfall increased to 1080.6 mm, which is approximately 30%
195 more than the average value and close to the maximum.

196 The following common traits can be identified from comparing the annual
197 meteorological conditions of DF1, DF2 and DF3. 1) One or two years before the
198 debris flows, the mean annual temperature elevated and the annual rainfall and
199 summer rainfall declined. The climate was in a "hot-dry" state. 2) As the temperature
200 gradually decreased, the annual rainfall returned to normal or increased, and the
201 "hot-wet" climate contributed to debris flow initiation (Lu and Li, 1989).

202 (2) Changing of glacier in Tianmo valley

203 In our research, remote image is collected to analyze the changing of glacier in
204 the source area during the past years. In order to eliminate the effect of snow cover,
205 images were taken in the thawing seasons when the snow cover is limited to enable an
206 easy detection of the glacier from snow. Besides, a bright cloud is still needed to show
207 the watershed clearly; however a difficult case ensues when the rainy season comes
208 in-between the thawing season when the atmosphere is often covered by thick cloud.
209 Further, in order to show glacier retreat and its impact on debris flows properly, the
210 images should be within similar time interval, like 3 years, before and after debris
211 flow events. As the high resolution images are rare to obtain and we could only collect
212 one SPOT image (Take by the satellite of Systeme Probatoire d'Observation de la
213 Terre with a space resolution of 5m) in 2008. To achieve consistency of the images,
214 we collected 5 TM images image (Taken by No. 4 or 5 thematic mapper carried on the
215 satellite Landsat with a space resolution of 30m), taken on Sep. 17th, 2000, Jul. 24th,
216 2003, Sep. 21st, 2006, Sep. 24th, 2009 and Aug. 4th, 2013, respectively.

217 Based on the 5 TM images, we classified the area as glacier, snow, bared land,
218 gully deposition and vegetation in time series (Figure 6), and the area of each is given
219 in Table 1. Figure 6 showed that deglaciation was taking place in Tianmo valley and
220 in particular, the eastern branch had experienced the sharpest deglaciation. In order to
221 show clearly the rapid rate of glacier retreat, a graph was plotted to show the changing
222 of glacier and the eastern branch in Figure 7.

223 Figure 7 shows that glacier in Tianmo valley had been in shrinkage since 2000 to
224 2013, with variation in glacier retreat rate. In 2000~2003, 2003~2006, 2006~2009 and
225 2009~2013, the glacier retreat rate in Tianmo valley corresponds to 0.02, 0.06, 0.027
226 and 0.0075km²/a and 0.0033, 0.01, 0.008 and 0.002 km²/a for the eastern branch.
227 According to these figures the largest glacier retreat rate was in 2003~2006, followed
228 by that in 2006~2009. It is important that glacier area at the beginning should be taken
229 into consideration to judge the changing rate of glacier. The glacier retreat rate is
230 normalized and the relative glacier retreat rate can be calculated based on their area

231 changing, which is defined as the retreat area of glacier in one year.

232 The relative glacier retreat rate are 11.30, 35.09, 17.43 and $5.17 \times 10^{-3} \text{km}^2/\text{a}/\text{km}^2$
233 during 2000~2003, 2003~2006, 2006~2009 and 2009~2013, respectively; whereas, it
234 is 20.83, 66.67, 66.67 and $20.83 \times 10^{-3} \text{km}^2/\text{a}/\text{km}^2$ for the eastern branch. These figures
235 show that the relative glacier retreat rate for the eastern branch had shrunk much more
236 sharply between 2000 ~2013.

237 In this research, TM images with 3 year intervals were applied can only get the
238 mean glacier retreat rate. As glacier retreat rate in the 3 three years could be either
239 high or low, field measurement of the nearby glacier is used to show the glacier retreat
240 condition before debris flows. Yang et al.(2015) had conducted field measurement of
241 No.94 Glacier in Parlung Zangbo Basin since 2006 and the field measurement
242 suggests it was in negative balance in 2006~2010(Figure 7). The negative balance
243 reached the maximal in 2009, followed by 2008 and 2006, indicating sharp
244 deglaciation in these three years.

245 When we combined the result of TM image and filed measurement of No. 94
246 Glacier, we observed that it is right before debris flows that glacier in Tianmo valley
247 experienced the sharpest deglaciation in 2006, 2008 and 2009, which was also
248 coincidental with the elevated mean annual air temperature (Figure 5).

249 **(3) Antecedent air temperature and rainfall process**

250 The air temperature in the source area can be obtained using the vertical decline
251 rate ($0.54^\circ\text{C}/100 \text{m}$). According to this method, the air temperature in the source area
252 was 9.8°C lower than that at the Bomi meteorological station. We collected the daily
253 temperature; that is the lowest temperature, the mean temperature and daily rainfall
254 from June to September in 2007 and 2010 (Figure 8).

255 According to Figure 8, the lowest air temperature was below 0 at the end of June,
256 2007. At the beginning of July, the air temperature started to rise quickly which
257 continued until early September when DF1 occurred, this demonstrates that the high
258 air temperature in July and August contributed to DF1.

259 According to Figure 8, the air temperature was high from early July to late

260 August, and another high air temperature period emerged in early September. When
261 DF2 occurred in late July the air temperature had reached the maximum for that year,
262 which suggests that the air temperature in early and middle July was responsible for
263 DF2. After DF2 occurred, the air temperature in August began to prepare for DF3.

264 Antecedent air temperature fluctuation includes the air temperature and its
265 duration. The air temperature and duration before debris flows are variable, making
266 them difficult to evaluate. The accumulation of positive air temperature is usually
267 applied to analyze the impact of air temperature on glacier melting (Rango and
268 Martinec, 1995), which can be expressed as:

$$269 \quad T_{PT} = \sum_{i=-n}^0 T_i (T_i > 0) \quad (1)$$

270 Where T_{PT} is the positive air temperature accumulation, °C and T_i is the
271 average daily air temperature; only $T_i > 0$ is included.

272 Because air temperature is successive, it is difficult to determine the beginning of
273 positive air temperature accumulation. Glacial tills can lessen the heat that penetrates
274 into them, and the low air temperature can only contribute to the upper thin layer;
275 moreover, freeze-thaw cycles exist when the lowest air temperature is less than 0°C.
276 From this point of view, the beginning of positive air temperature accumulation is
277 defined as the time at which the lowest air temperature exceeds 0°C for two or three
278 successive days and the following days was higher than 0°C or the last debris flow.

279 Based on the above method, we can deduce that the positive air temperature
280 accumulation began when the lowest air temperature exceeded 0°C for several
281 successive days, starting on June 28th, 2007 and June 9th, 2010 corresponding to DF1
282 and DF2, respectively, and on July 26th, 2010 for DF3, following DF2. The duration
283 and T_{PT} were calculated for each debris flow event, the result was 69 days and
284 517.9°C, 47 days and 332.1°C, 42 days and 320.4°C (Figure 8) for DF1, DF2, and
285 DF3, respectively. The result showed that T_{PT} for DF1 is much larger than the other
286 two, and which is coincidence to the fact that there was that there was no debris flows

287 in the past dozens of years and extraordinary external forces such as larger T_{PT} is
288 required to destroyed the long-term balance the the fully recharged channel could be
289 another reason.

290 **(4) Triggering conditions**

291 The continuous nature of the air temperature limits the possibility for debris
292 flows triggered by a sole abrupt increase in air temperature; and since the previous air
293 temperature trend cannot be neglected, it is of no sense to study air temperature
294 triggers.

295 Antecedent rainfall is a factor that favours debris flows. In our analysis, the
296 rainfall over the three days preceding a debris flow event is given in Figure 9.

297 Before DF1, the air temperature was high, and continued through July and
298 August. The T_{PT} reached 517.9°C. According to the local forest guard, an isolated
299 convective storm occurred prior to DF1 though no rainfall was recorded at the Bomi
300 meteorological station or in the downstream area at that time. In Figure 9, as the
301 rainfall right before DF1 occurred was not recorded by Bomi metrological station, we
302 added to the rainfall intensity (about 5 mm/h according to the description of the forest
303 guard) before DF1 to account for the storm, which might not reflect the real rainfall
304 process. We can therefore conclude that this isolated convective storm initiated DF1,
305 while the long-term high air temperature trend had paved the road for DF1.
306 Considering a large deglaciaded area, several other periglacial debris flows
307 simultaneously also occurred near Tianmo Valley (Deng et al, 2013), which suggests
308 the advantageous meteorological conditions for debris flow initiation.

309 DF2 took place when the air temperature reached the peak in 2010. The thaw
310 season began in the middle of June, and the T_{PT} reached 332.1°C. On July 24th, one
311 day before DF2, the air temperature reached the maximum value for that year. The
312 rainfall record at the Bomi meteorological station shows that there had been no
313 rainfall several days preceding DF2, and the local citizens also did not observe any
314 rain either. The trigger of DF2 was likely the continuous percolation of melt-water

315 due to the long term rising air temperature.

316 According to field interviews, several debris flows of small magnitude had also
317 occurred before DF3. The air temperature decreased in late August but increased to
318 another high peak before DF3, and the T_{PT} reached 320.4°C. Rainfall began 2 days
319 prior to DF3 and was steady the entire day before DF3. According to the rainfall trend
320 at the Bomi meteorological station, the rapid increase in rainfall intensity started 4
321 hours before DF3 and reached 3.8 mm/h, which was responsible for the initiation of
322 DF3.

323 **4. Discussion**

324 Debris flows initiation is the process when water source provokes the movement
325 of soil sediment. In this research, we found that the three debris flows were triggered
326 by high air temperature and rainfall in DF1, high air temperature in DF2, and rainfall
327 in DF3 respectively. When we analyzed the date and the triggers for these events,
328 various questions came to mind that gave reasons to doubts: 1) Why debris flows did
329 not occur in 2006 or 2009 when deglaciation reached its peak and more ice melt water
330 was present; 2) Why DF1 and DF3 occurred in September when the air temperature
331 and the ice melt water was decreasing; 3) Why was there is no large scale debris flows
332 triggered by the previous heavier storm. It makes us believe that the impact of water
333 source on the magnitude and frequency of debris flows is quite low, or there could be
334 much more debris flows; and instead, soil source, including its magnitude and activity,
335 should be the predominate controller, just as Jakob et al., (2005) pointed out that the
336 recharge of channel should be the prerequisite for debris flows. However, in most
337 situations we cannot reach the source area to detect the soil source and the high-tech
338 remote sensing can just distinguish the boundary of soil source. In the periglacial area
339 where the glacial till is often covered by glacier or everlasting snow, changing of soil
340 source seems to be of high difficulty to detect. In this research, we try to combine the
341 meteorological condition and the literatures to discuss the probable variation of glacial
342 tills before debris flows.

343 **(1) Variation of glacial till in annual years**

344 Climate warming is a global trend (IPCC, 2013), and the Tibetan Plateau, as the
345 third pole, is no exception. According to our statistics, the air temperature in Bomi
346 County has increased by 1.5° in the last 45 years (1970~2014). Glacier retreat induced
347 by climate warming has been widely accepted, and recent research suggests the
348 weaker Indian monsoon could be another reason (Yao et al, 2012). Glaciers are
349 always located in concave ground and cover a large amount of glacial tills. Glacial
350 pressure can generate normal stress vertical to the slope, which can strengthen the
351 slope stability. The effect of glaciers on slope stability is called glacial debuttreasing
352 (Cossart et al, 2008). As deglaciation continues, the result could lead to exposure of
353 the frozen glacial tills (Figure 10, A to B) and smaller glacial debuttreasing.

354 The retreat of glaciers and glacial tills with climate warming is quite different.
355 Deglaciation is accompanied by melting of internal ice particles. The melt of internal
356 ice particles can produce active surface layer which can obstruct heat flux from
357 penetrating into the deep layer, result into the melting of internal ice particles lagging
358 behind glacial retreat (Hagg et al, 2008). As strong heat gradient is existed at the
359 surface while quite limited in deep layers, glacial tills with thicker depth always has a
360 relatively slower ablation rate, and the ablation rate of glaciers and internal ice
361 particles can enjoy the same value at the glacier surface close to the moraine slope.
362 The newly formed bared glacial till is frozen with high ice content, the cohesion of the
363 ice particles renders the bared glacial till with high shearing strength and stability and
364 only the surface layer is of high activity. Therefore, we often see many bare moraine
365 slopes near glaciers, for this reason there were no debris flows of large magnitude in
366 2006 and 2009 when glacier retreat reached the maximal.

367 **(2) Variation of glacial till in antecedent days**

368 After the long term cold winter, the whole glacial tills would become frozen. If
369 the regressive glacier was not recovered in the winter, the glacial tills would often be
370 covered by snow. As air temperature increases again, the surface snow would melt

371 first, followed by the internal ice particles. The thawing of internal ice particles would
372 induces a series of changes in the glacial till, which include the following: 1) the
373 thawing will break the bonds of ice particles and increase the instability between ice
374 cracks (Ryzhkin and Petrenko, 1997; Davies et al, 2001); 2) the sharp air temperature
375 fluctuation in high alpine mountainous areas induces a repeated cycle of expansion
376 and contraction in the glacial till that can destroy the mass structure to some extent; 3)
377 the seepage of ice melt-water can deliver fine-grained sediments that were formerly
378 frozen in the ice matrix (Rist, 2007); and 4) the ice melt-water can result in a higher
379 water content and pore water pressure (Christian et al, 2012). These changes in glacial
380 till can sharply decline the soil strength, shifting to an active mass from the uncovered
381 and frozen moraine (Figure 10, B to C). Because the heat conduction in glacial till is
382 quite slow, this process may last for a very long time and also requires a high
383 antecedent air temperature.

384 Heat conduction via the percolation of rainfall and ice melt-water can amplify
385 the depth of active of glacial till (Gruber and Haeberli, 2007), whereas the shelter of
386 surface glacial till can hinder the heat flux from penetrating into the deep layer. At a
387 low air temperature, the heat flux should be constrained to the surface layer, and a
388 large heat gradient due to a high air temperature would contribute much more to the
389 heat flux and ice melt in the deep mass, meaning that the long-term effect of a high air
390 temperature can amplify the active glacial till (Åkerman et al, 2008), under which lies
391 frozen glacial till with a high ice content. The activity of glacial till variations with
392 depth, high in the surface and low in the deep layers, and landslide failure can take
393 place on glacial till slopes in a retrogressive manner, coinciding with long-term air
394 temperature fluctuations although the glacial till is significantly unlimited in
395 deglaciation areas.

396 **(3) Failure of glacial tills**

397 Failure of glacial could be diversity. Active glacial till slopes with low strength
398 are usually vulnerable, and their failure can occur when the air temperature is above
399 0°C (Arenson and Springman, 2005). Either rainfall, the seepage flow of glacier or ice

400 particle melt-water could percolate the tills and trigger the failure (Figure10, C to D).
401 This kind is called the shallow landslide type, and the failure mechanism lies in the
402 ablation of internal ice particles and the percolation of melt-water can decrease the
403 soil strength at first (Arenson and Springman, 2005; Decaulne et al, 2005); later, the
404 subsequent rapid percolation of melt-water or rainfall can saturate the glacial till,
405 decrease soil suction and shearing strength and then trigger the shallow landslide
406 failure (Springman et al, 2003; Decaulne and Sæmundsson, 2007; Chiarle et al, 2007).
407 Whether the failure can induce debris flows is still dependent on the ability that it can
408 entrain the debris layer, otherwise, it can deposit and charge the channel.

409 Another kind of failure can take place by the increased water stream that entrain
410 sediments and forms a solid-liquid wave if the channel is charged with loose ravel.
411 This kind of water stream could be the combination of the three factors, including
412 rainfall, melting ice or the overflow when the glacier collapse falling down into the
413 downwards water pool. The runoff can generate debris flows when a peaked runoff
414 flow over debris deposits(Kean et al., 2013; Gregoretti et al., 2016) and pose
415 hydrodynamic forces acting on the surface elements of the debris layer(Tognacca et al.
416 2000, Gregoretti, 2000). The concentration of runoff in the channel bottom causes
417 erosion of the debris surface layer and then extends to the layers below with whole or
418 partial mobilization of the bed material. The inclusion of bed material in the water
419 stream generates debris flow (Gregoretti, 2008).

420 The fluctuation of air temperature within a specific low range can result into
421 limited seepage flow. glacier in one valley is limited, it is unlikely for failure to be
422 triggered by the limited ice melt water in short-term increases of air temperature;
423 instead, prolong air temperature increases it is needed to generate more water flow.
424 Rainfall can initiate debris flows from active glacial tills with a mechanism similar to
425 that of storm-induced debris flows in non-glacier areas (Iverson et al, 1997;
426 Springman et al, 2003; Sassa and Wang, 2005; Gregoretti, 2008; Kean et al., 2012). In
427 the European Alps, periglacial debris flows are mainly provoked by rainfall, which is
428 also related with air temperature fluxes (Stoffel et al, 2011). The portion of rainfall
429 and air temperature required for debris flows triggering could be negative. Air

430 temperature increase causes melting and water runoff, and the rainfall needed for
431 providing the percolating flows or exact critical discharge for debris flow triggering
432 would be much less. Beside, the required rainfall, like the rainfall intensity and
433 duration, may also require other preconditions, such as the distribution of glaciers and
434 frozen glacial tills and the terrain of the source area to enhance the debris flow
435 (Lewkowicz and Harris, 2005).

436 The three debris flow events possess similar annual meteorological conditions,
437 except that the positive air temperature accumulation prior to DF1 was significantly
438 larger. DF1 occurred at the end of a prolonged period of high air temperature, prior to
439 this, there were instances of failure but no large-scale debris flows. On July 25th 2010
440 when the daily rainfall particularly reached 20.7 mm, no debris flows were generated
441 because thick active glacial till was still lacking after small failure events. In 2010, the
442 largest daily rainfall occurred on June 7th, accounting for 37.5 mm, at the beginning of
443 an air temperature increase when the glacial till was frozen and had low activity. The
444 lack of glacial till activity was the likely cause of the absence of debris flows. On
445 August 23rd, the daily rainfall was 20.3 mm, the antecedent air temperature
446 accumulation dated from DF2, and the active glacial till was still under development.
447 On September 6th, the antecedent positive air temperature accumulation was smaller,
448 and a low air temperature had emerged previously; however, the high rainfall intensity
449 supplemented this lack of prolonged high air temperature.

450 **5. Conclusion**

451 Climate changes have serious effects on high mountainous areas, and mass
452 movement of sediments such as periglacial debris flows is increasingly frequent.
453 Prolonged increases in the mean annual air temperature are regarded as very
454 favourable for periglacial debris flows. In particular, the annual “hot-dry” weather
455 condition one or two year earlier was responsible for the three debris flow events in
456 Tianmo valley. Debris flow is usually not initiated in the year when the mean annual
457 air temperature spikes as melting of internal ice particles lags behind the glacial
458 retreat result from the prolong air temperature rise.

459 Glacial till is unlimited in the deglaciated area, while its activity relies on glacial
460 retreat and internal ice particle melting. Changing of glacial tills induced by
461 increasing air temperature is the first step of periglacial debris flows comparing with
462 the storm induced debris flows in non-glacier area, during which the varied air
463 temperature condition with different factor drives the changing and temperature series
464 can remove glaciers, produce bared glacial till and enhance the activity step by step.

465 It is difficult to observe the changes of glacial till in source areas of debris flow,
466 and the analysis of the phase conversion of glacial till in this research is based on the
467 triggering conditions and other literatures. Indeed, the meteorological conditions, such
468 as the antecedent air temperature and meteorological triggers that drive the phase
469 conversion are partly overlapped and difficult to distinguish. In the first study, we
470 hope to distinguish the effect of each meteorological condition and more detail study
471 should be done in further research.

472 **Acknowledgements:** This research was supported by the National Natural Science Foundation
473 of China (grant No. 41190084, 41402283 and 41371038) and the “135” project of IMHE, CAS.
474 We wish to acknowledge the editors in the Natural Hazards and Earth System Science Editorial
475 Office and the anonymous reviewers for constructive comments, which helped us in improving the
476 contents and presentation of the manuscript.

477 **References**

- 478 Åkerman, H. J., and Johansson, M.: Thawing permafrost and thicker active layers in sub-Arctic
479 Sweden. *Permafrost Periglac*, 19(3), 279-292, 2008.
- 480 Arenson, L. U., and Springman, S. M.: Mathematical descriptions for the behaviour of ice-rich
481 frozen soils at temperatures close to 0 °C. *Can Geotech J*, 42(2), 431-442, 2005.
- 482 Chen, N. S., Zhou, H. B., and Hu, G. S.: Development Rules of Debris Flow under the Influence
483 of Climate Change in Nyingchi. *Adv Clim Change Res*, 7(6), 412-417, 2011. (In Chinese)
- 484 Chen, R.: Initiation and the critical condition of Glacial debris flow. Master thesis. Institute of
485 Mountain Hazards and Environment, Chinese Academic of Sciences. P19, 1991.
- 486 Cheng, Z. L., Wu, J. S., and Geng, X.: Debris flow dam formation in southeast Tibet. *J Mt Sci*,
487 2(2), 155-163, 2005.

488 Chiarle, M., Iannotti, S., Mortara, G., and Deline, P.: Recent debris flow occurrences associated
489 with glaciers in the Alps. *Global Planet Change*, 56:123-136, 2007.

490 Christian, B., Philipp, F., and Hansruedi, S.: Thaw-Consolidation Effects on the Stability of Alpine
491 Talus Slopes in Permafrost. *Permafrost Periglac*, 23, 267-276, 2012.

492 Cossart, E., Braucher, R., Fort, M., Bourlès, D. L., and Carcaillet, J.: Slope instability in relation to
493 glacial debuitressing in alpine areas (Upper Durance catchment, southeastern France):
494 Evidence from field data and ¹⁰Be cosmic ray exposure ages. *Geomorphology*, 95, 3-26,
495 2008.

496 Cruden, D. M., and Hu, X. Q.: Exhaustion and steady state models for predicting landslide hazards
497 in the Canadian Rocky Mountains. *Geomorphology*, 8, 279-285, 1993.

498 Davies, M., Hamza, O., and Harris, C.: The effect of rise in mean annual temperature on the
499 stability of rock slopes containing ice-filled discontinuities. *Permafrost Periglac*, 12(1),
500 137-144, 2001.

501 Deng, M. F., Chen, N. S., Ding, H. T., and Zhou, C. C.: The Hydrothermal Condition of 2007
502 Group-occurring Debris Flows and Its Triggering Mechanism in Southeast Tibet. *J Nat Disa*,
503 22(4), 128-134, 2013. (In Chinese)

504 Decaulne, A., and Sæmundsson, T.: Spatial and temporal diversity for debris-flow meteorological
505 control in subarctic oceanic periglacial environments in Iceland. *Earth Surf Proc Land*,
506 32(13), 1971-1983, 2007.

507 Decaulne, A., Sæmundsson, T., Petursson, O.: Debris flows triggered by rapid snowmelt in the
508 Gleidarhjalli area, northwestern Iceland. *Geografiska Annaler*, 87A, 487-500, 2005 .

509 Evans, S. G., Tutubalina, O., Drobyshev, V. N., Chernomorets, S. S., McDougall, S., Petrakov, D.
510 A., and Hungr, O.: Catastrophic detachment and high-velocity long-runout flow of Kolka
511 Glacier, Caucasus Mountains, Russia in 2002. *Geomorphology*, 105(3), 314-321, 2009.

512 Fischer, L., Purves, R. S., Huggel, C., Noetzli, J., and Haeberli, W.: On the influence of
513 topographic, geological and cryospheric factors on rock avalanches and rockfalls in
514 high-mountain areas. *Nat Hazard Earth Sys*, 12(1), 241-254, 2012.

515 Ge, Y. G., Cui, P., Su, F. H., Zhang, J. Q., Chen, X. Z.: Case history of the disastrous debris flows
516 of Tianmo Watershed in Bomi County, Tibet, China: Some mitigation suggestions *J Mt Sci*,
517 11(5), 1253-1265, 2014.

518 Gregoretti, C.: The initiation of debris flow at high slopes: experimental results. *Journal of*
519 *Hydraulic Research*, 38(2): 83-88, 2000.

520 Gregoretti, C., Degetto, M., Bernard, M., Crucil, G., Pimazzoni, A., De, V.G., Berti, M., Simoni,
521 A., Lanzoni, S.: Runoff of small rocky headwater catchments: Field observations and

522 hydrological modeling. *Water Resources Research*, 52(8), doi: 10.1002/2016WR018675,
523 2016.

524 Gregoretti, C., Fontana, G.D.: The triggering of debris flow due to channel-bed failure in some
525 alpine headwater basins of the Dolomites: Analyses of critical runoff, *Hydrological processes*,
526 22(13): 2248-2263, 2008. Gruber, S., and Haeberli, W.: Permafrost in steep bedrock slopes
527 and its temperature-related destabilization following climate change. *J Geophys Res*, 112,
528 (F02S18), 2007.

529 Guzzetti, F., Peruccacci, S., Rossi, M., and Stark, C. P.: The rainfall intensity-duration control of
530 shallow landslides and debris flows: an update. *Landslides*, 5, 3-17, 2008.

531 Harris, C., Arenson, L. U., Christiansen, H. H., Etzelmüller, B., Frauenfelder, R., Gruber, S., ...
532 and Isaksen, K.: Permafrost and climate in Europe: Monitoring and modeling thermal,
533 geomorphological and geotechnical responses. *Earth Sci Rev*, 92, 117-171, 2009.

534 Harris, C., and Lewkowitz, A. G.: An analysis of the stability of thawing slopes, Ellesmere Island,
535 Nunavut, Canada. *Can Geotech J*, 37(2), 449-462, 2002.

536 IPCC. Summary for policymakers. Working group I contribution to the IPCC Fifth assessment
537 report climate change 2013: the physical science basis. Cambridge, UK: Cambridge
538 University Press, 2013.

539 Iverson, R. M., Reid, M. E., and LaHusen, R. G.: Debris-flow mobilization from landslides. *Annu*
540 *Rev Earth Pl Sci*, 25(1), 85-138, 1997.

541 Jakob, M.: A size classification for debris flows. *Engineering geology*, 79(3), 151-161, 2005.

542 Jakob, M., Bovis, M., and Oden, M.: The significance of channel recharge rates for estimating
543 debris-flow magnitude and frequency, *Earth Surf. Proc. Land.*, 30, 755-766, 2005.

544 Li, Q. Y., and Xie, Z. C.: (2006) Analysis on the characteristics of the vertical lapse rates of
545 temperature. Taking Tibetan Plateau and its adjacent area as an example. *J Shihezi University*
546 *(Natural Science)*, 24 (6), 719-723, 2006. (In Chinese).

547 Kean, J. W., McCoy, S. W., Tucker, G. E., Staley, D. M., and Coe, J. A.: Runoff generated debris
548 flows: observations and modeling of surge initiation, magnitude, and frequency. *J Geophys*
549 *Res*, 118, 2190-2207, 2013.

550 Korup, O., and Clague, J. J.: Natural hazards, extreme events, and mountain topography.
551 *Quaternary Sci Rev*, 28, 977-990, 2009.

552 Lewkowitz, A. G., and Harris, C.: Frequency and magnitude of active-layer detachment failures in
553 discontinuous and continuous permafrost, northern Canada. *Permafrost Periglac*, 16(1),
554 115-130, 2005.

555 Liu, J. J., Cheng, Z. L., and Su, P. C.: The relationship between air temperature fluctuation and

556 Glacial Lake Outburst Floods in Tibet, China. *Quatern Int*, 321, 78-87, 2014.

557 Liu, Y.: Research on the typical debris flows chain based on RS in Palongzangbu Basin of Tibet.

558 Chengdu University of Science and Technology, Master thesis, 2013. (In Chinese)

559 Lu, R. R., and Li, D. J.: Ice-Snow-Melt Debris Flows in the Dongru Longba, Bomi county, Xizang.

560 *J Glac Geocry*, 11(2), 148-160, 1989. (In Chinese)

561 McColl, S. T.: Paraglacial rock-slope stability. *Geomorphology*, 153-154, 1-16, 2012.

562 Noetzli, J., Gruber, S., Kohl, T., Salzmann, N., and Haeberli, W.: Three-dimensional distribution

563 and evolution of permafrost temperatures in idealized high-mountain topography. *J Geophys*

564 *Res*, 112, F02S13, 2007.

565 Rahardjo, H., Leong, E. C., and Rezaur, R. B.: Effect of antecedent rainfall on pore-water pressure

566 distribution characteristics in residual soil slopes under tropical rainfall. *Hydrol Process*,

567 22(4), 506-523, 2008.

568 Rango, A., and Martinec, J.: Revisiting the degree-day method for snowmelt computations.

569 *JAWRA Journal of the American Water Resources Association*, 31(4), 657-669, 1995.

570 Rist, A.: Hydrothermal processes within the active layer above alpine permafrost in steep scree

571 slopes and their influence on slope stability. Unpublished PhD thesis, Swiss Federal Institute

572 for Snow and Avalanche Research and University of Zurich, Zurich, 168 pp, 2007.

573 Ryzhkin, I. A., and Petrenko, V. F.: Physical mechanisms responsible for ice adhesion. *J Phys*

574 *Chem B*, 101(32), 6267-6270, 1997.

575 Sassa, K., and Wang, G. H.: Mechanism of landslide-triggered debris flows: Liquefaction

576 phenomena due to the undrained loading of torrent deposits[M]//*Debris-flow hazards and*

577 *related phenomena*. Springer Berlin Heidelberg. 81-104, 2005.

578 Sattler, K., Keiler, M., Zischg, A., and Schrott, L., On the connection between debris flow activity

579 and permafrost degradation: a case study from the Schnalstal, South Tyrolean Alps,

580 Italy. *Permafrost Periglac*, 22(3), 254-265, 2011.

581 Schneuwly-Bollschweiler, M., and Stoffel, M.: Hydrometeorological triggers of periglacial debris

582 flows in the Zermatt valley (Switzerland) since 1864. *J Geophys Res*, 117, F02033, 2012.

583 Shang, Y. J., Yang Z. F., Li, L., Liu, D. A., Liao, Q., Wang, Y.: A super-large landslide in Tibet in

584 2000: background, occurrence, disaster, and origin. *Geomorphology*, 54(3), 225-243, 2003.

585 Springman, S. M., Jommi, C., and Teyssere, P.: Instabilities on moraine slopes induced by loss of

586 suction: a case history. *Géotechnique*, 53(1), 3-10, 2003.

587 Stoffel, M., Bollschweiler, M., and Beniston, M.: Rainfall characteristics for periglacial debris

588 flows in the Swiss Alps: past incidences–potential future evolutions. *Climatic Change*,

589 105(1-2), 263-280, 2011.

590 Stoffel, M., and Huggel, C.: Effects of climate change on mass movements in mountain
591 environments. *Prog Phys Geog*, 36(3), 421-439, 2012.

592 Takahashi, T.: *Debris flow: mechanics, prediction and countermeasures*. CRC Press, 2014.

593 The Ministry of Land and Resources P. R. C.: *China Geological Hazard Bulletin*(September
594 edition), 2010.

595 Tognacca, C., Bezzola, G.R., Minor, H. E., Threshold criterion for debris-flow initiation due to
596 channel bed failure. In: Wiczorek, G.F. (Ed.), *Proceedings Second International Conference*
597 *on Debris Flow Hazards Mitigation: Mechanics. Prediction and Assessment*, Taipei, pp.
598 89-97, 2000.

599 Yao, T. D., Thompson, L., Yang, W., Yu, W., Gao, Y., Guo, X., ... and Pu, J.: Different glacier
600 status with atmospheric circulations in Tibetan Plateau and surroundings. *Nature Climate*
601 *Change*, 2(9), 663-667, 2012.

602 Yang, W., Guo, X., Yao, T., Zhu, M., and Wang, Y. Recent accelerating mass loss of southeast
603 Tibetan glaciers and the relationship with changes in macroscale atmospheric
604 circulations. *Clim Dynam*, 1-11, 2015.

605 Yang, W., Yao, T., Xu, B., Ma, L., Wang, Z., and Wan, M. Characteristics of recent temperate
606 glacier fluctuations in the Parlung Zangbo River basin, southeast Tibetan Plateau. *Chinese*
607 *Sci Bull*, 55(20), 2097-2102, 2010.

608 Yuan, G.X., Ding, R. W., Shang, Y. J., Zeng, Q. L.: Genesis of the Quaternary accumulations along
609 the Palong section of the Sichuan-Tibet Highway and Their Distribution Regularities.
610 *Geology and Exploration*, 48(1), 170-176, 2012. (In Chinese)

611

612

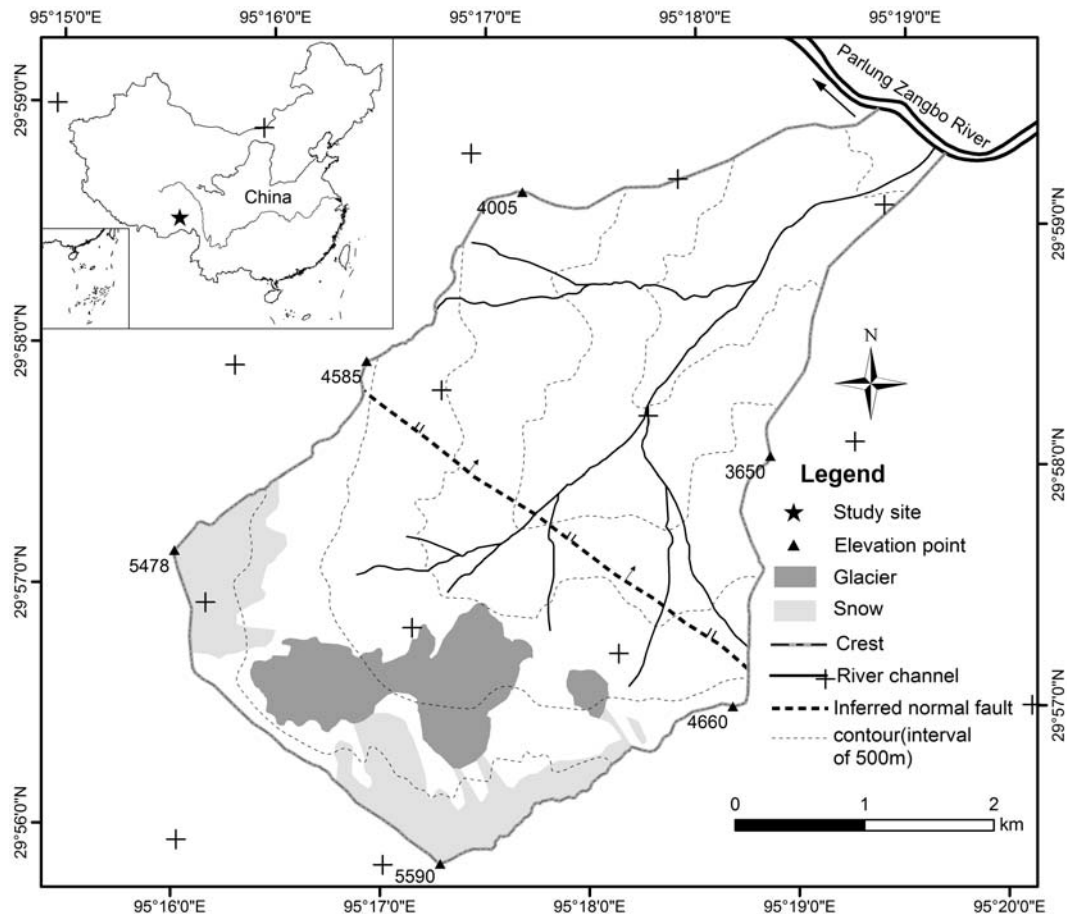
613 Table 1 Changing of glacier, snow, bared land, gully deposition and vegetation in Tianmo valley

Year	Glacier (km ²)	Glacier(eastern branch) (km ²)	Snow (km ²)	Bared land (km ²)	Gully deposition (km ²)	Vegetation (km ²)
2000	1.77	0.16	2.13	2.80	0.44	10.46
2003	1.71	0.15	2.44	2.54	0.44	10.48
2006	1.53	0.12	2.68	2.44	0.44	10.55
2009	1.45	0.096	2.81	3.03	0.47	9.90
2013	1.42	0.088	1.74	3.83	0.51	10.17

614

615 Table 2 Basic information of the debris flows in Tianmo and the nearby valleys

No.	Name	Coordinates	Basin area (km ²)	Glacier area (in 2006) (km ²)	Date	Size class
1	Tianmo valley	29°59'N 95°19'E	17.74	1.53	4 Sep. 2007	6
					25 Jul. 2010	5
					6 Sep. 2010	5
2	Kangbu valley	30°16'N 94°48'E	48.7	1.06	4 Sep. 2007	3
3	Xuewa valley	29°57'N 95°23'E	33.22	0.95	4 Sep. 2007	2
4	Baka valley	29°53'N 95°33'E	22.15	2.46	7 Sep. 2007	3
5	Jiaqing Valley	30°16'N 94°49'E	15.51	1.12	9 Sep. 2007	3



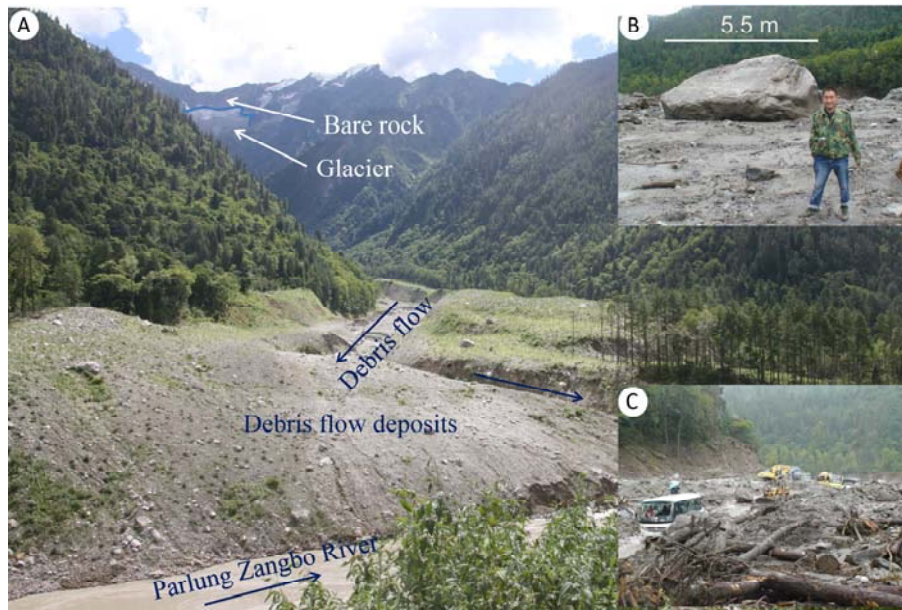
616
617

Figure 1 Location and basic information of Tianmo Valley



618
619

Figure 2 Overview of the valley from the channel(in 2014)

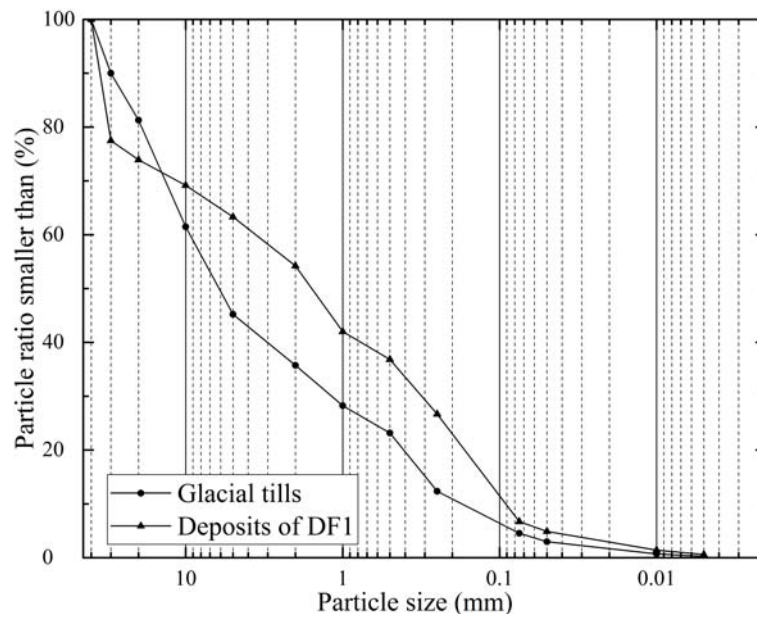


620

621 Figure 3 DF1 in 2007(A. Overview of Tianmo debris flows from the downstream area; B& C.

622

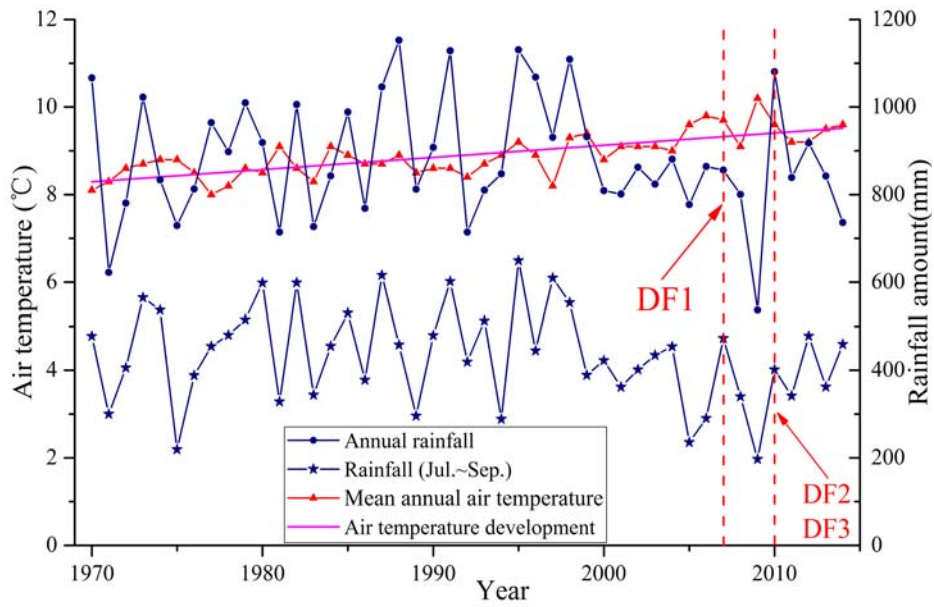
Boulder and debris flow deposits on the north side of the Parlung Zangbo River)



623

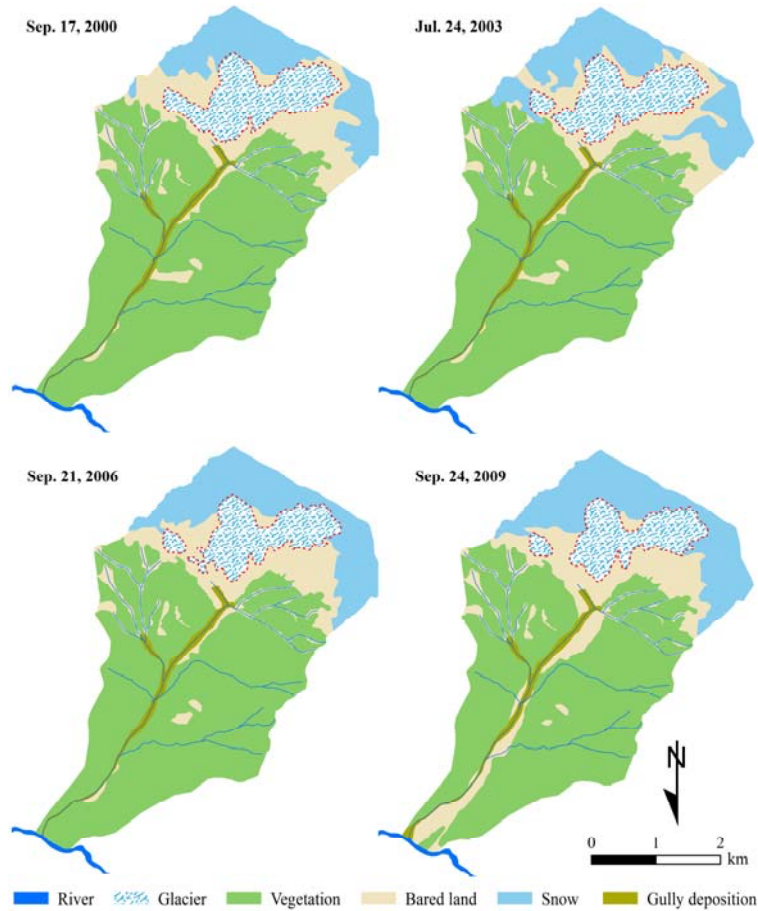
624

Figure 4 Particle size distributions of the glacial tills and debris flow deposits



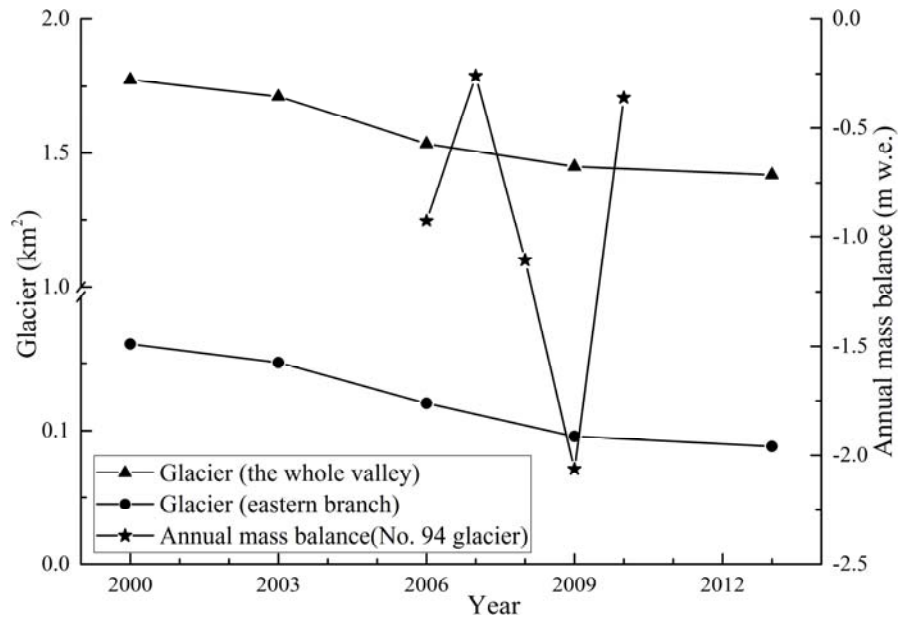
625
626

Figure 5 Variation of the mean annual air temperature and rainfall in Bomi, 1970 to 2014



627
628
629
630

Figure 6 Distribution and changing of glacier, snow, bared land, gully deposition and vegetation in Tianmo valley

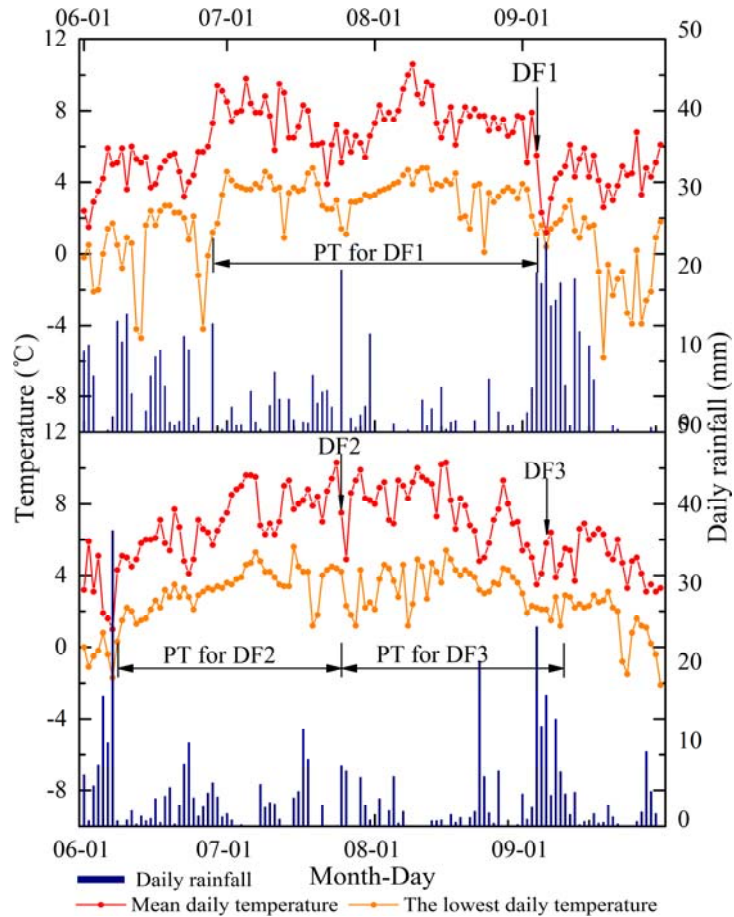


631

632

633

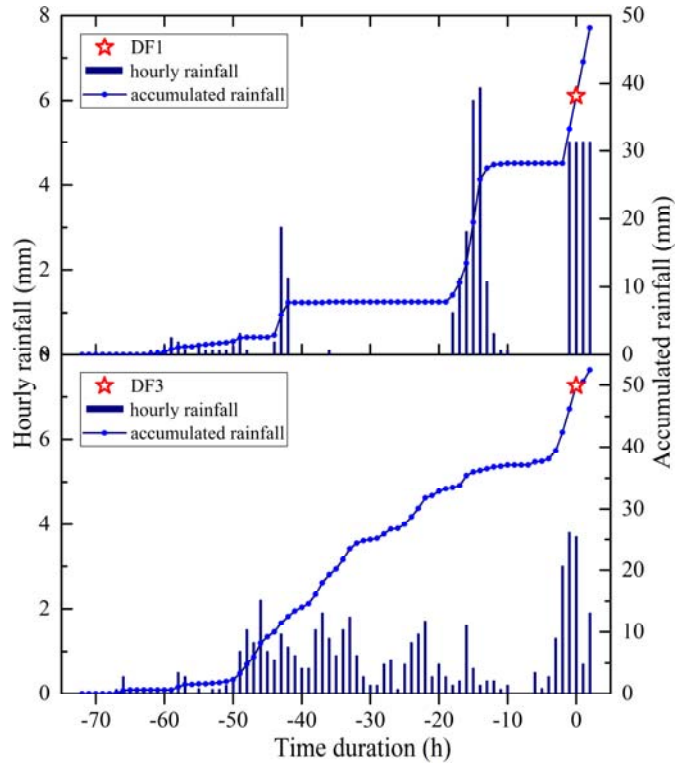
Figure 7 Changing of glacier via time and the measured annual mass balance for the Parlung No. 94 Glacier (mass balance is edited by Yang et al.(2015))



634

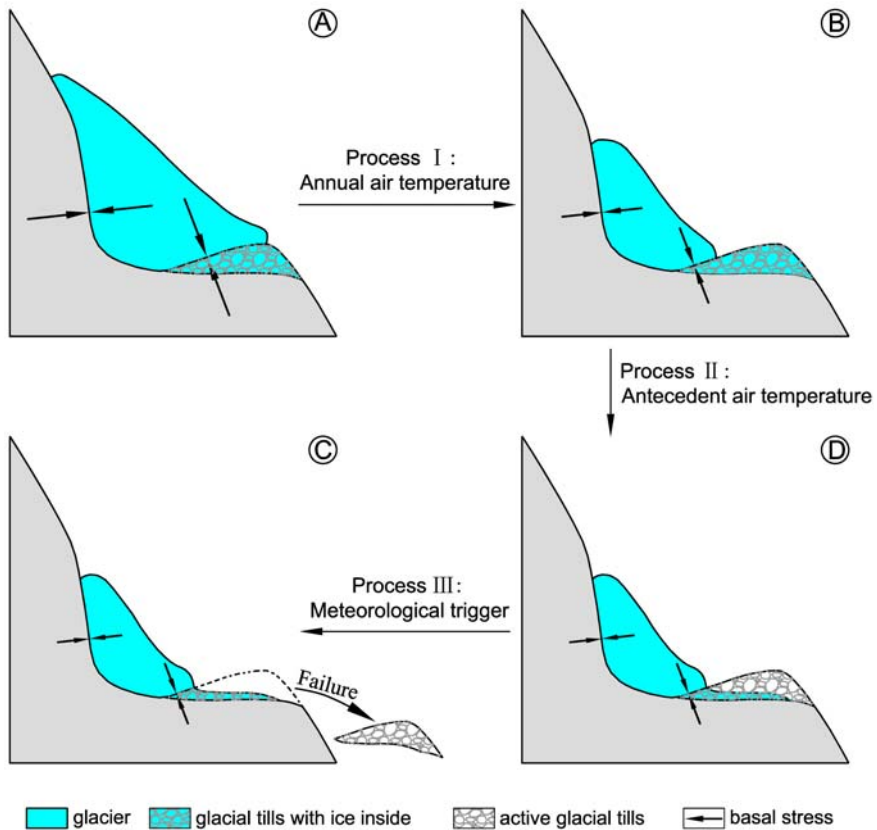
635

Figure 8 Air temperature and rainfall before and after DF1, DF2 and DF3



636

637 Figure 9 Variation of the rainfall accumulation prior to DF1 and DF3 (no rainfall before DF2)



638

639 Figure 10 Changes in a glacier and frozen glacial till before periglacial debris flow initiation(A:

640 glacial covered glacial tills; B: uncovered and frozen glacial tills; C: active glacial tills; D: failure

641

of glacial tills)